Digest Journal of Nanomaterials and Biostructures Vol. 7, No. 2, April - June 2012, p. 717 - 727

MECHANICAL CHARACTERIZATION OF DEFORMED CARBON NANOTUBES

MIR MASOUD SEYYED FAKHRABADI*, AKBAR ALLAHVERDIZADEH, VAHID NOROUZIFARD, BEHNAM DADASHZADEH
Karaj Branch, Islamic Azad University, Karaj, Iran

This paper investigates the mechanical behaviors of deformed carbon nanotubes including elastic, buckling and vibrational properties. The effects of stretching, twisting, bending and elliptic distortions are studied on the behaviors of the deformed carbon nanotubes. In both buckling and vibrational studies, two cantilever and doubly clamped boundary conditions are considered. The critical buckling loads and vibrational natural frequencies of the deformed carbon nanotubes and their corresponding mode shapes are presented in this paper. The well-known molecular mechanics approach is applied to model and investigate the mentioned properties.

(Received February 27, 2012; Accepted May 22, 2012)

Keywords: Carbon nanotube, Deformation, Elasticity, Vibration, Buckling.

1. Introduction

Nanotechnology as one of the most modern technologies has attracted many researchers all over the world to study the different aspects of nanosystems and nanostructures. Among various nanostructures, carbon nanotube (CNT) has an influential role in this technology due to its remarkable mechanical, electrical, thermal and chemical properties. This nanostructure has been employed in different fields including nanomaterial, nanoelectronics and nanomechanics during recent decades [1-3] Due to these extensive applications, its modeling and analysis in various conditions are more demanded.

The mechanical behaviors of the CNTs in their normal geometric conditions were researched well [4-10]. In general, researchers applied different methods such as molecular dynamics, molecular mechanics and continuum modeling to analyze the nanostructures. Some examples of the mentioned approaches are the following three papers. Legoas *et al*. used molecular dynamics method to simulate gigahertz CNT oscillators [11]. In another research, Li and Chou analyzed the vibrational behaviors of the CNTs as nanomechanical resonators using molecular mechanics [12]. They presented the natural frequencies and mode shapes of the single and double walled CNTs in two armchair and zigzag chiralities. Lastly, as an example for continuum modeling of the CNTs, Li and Chang applied classical continuum beam theories to investigate the possibility of using CNTs as tunable dual frequency oscillators composed of a cantilever inner tube and a short outer tube [13].

Applications of the CNTs in different conditions require studying their behaviors under the effects of different parameters. Mahdavi *et al*. presented nonlinear vibration of a single-walled CNT embedded in a polymer composite [14]. They analyzed the effects of van der Waals forces on the nonlinear behaviors of the CNT-based nanocomposites. In another paper, a similar research was conducted by Lee and Chang. They investigated the vibration of a single-walled CNT embedded in an elastic medium and conveying viscous fluid [15]. In their study, the surrounding elastic medium was modeled by some springs attached to the CNT and the results of shifting in frequencies for different flow properties such as different velocities, viscosities, and different aspect ratios were reported.

* *Corresponding author: msfakhrabadi@gmail.com ; mfakhrabadi@ut.ac.ir*

One of the main applications of the CNTs is their utility as nanomechanical sensors which were studied by some researchers. Li *et al*. reviewed the sensors and actuators based on the CNTs and their composites [16]. Charge distribution in the CNTs and their electromechanical actuation, failure due to the charges and the electrical conductivity of the CNTs were reviewed completely in the mentioned article. On the other hand, Tooski theoretically studied the application of the CNTs as gas sensors [17]. He investigated microwave absorption properties of the CNTs under different gas pressures using a combination of fluid and perturbation theories.

Nosrati *et al*. applied the first principle method to study the electronic properties of the functionalized CNTs [18]. In this paper, they investigated the electronic and structural properties of functionalized semiconducting and metallic single-walled CNTs using spin-polarized density functional theory. The results showed that in metallic and semiconducting CNTs with odd number of functional groups, an additional acceptor level was near the Fermi level but the systems functionalized with two groups retained their original properties. The CNTs with Y-junctions are relatively newly discovered nanostructures requiring much research and scientific attentions. Yazdani and Bahrami analyzed some physico-chemical properties of these nanostructures [19]. They determined their edge frustration number of structural models via proposing a novel approach.

In another research, Khan *et al*. fabricated a multi-walled CNT film catalyzed by cobalt for carbon mono-oxide gas sensing [20]. It was synthesized on silicon oxide grown silicon substrate using low pressure chemical vapor deposition. This paper and several other papers showed the possibility of the CNT applications in sensing.

The above descriptions related to the applications of the CNTs in different fields and working conditions show that their deformations in the different applications are inevitable. Therefore, their analysis in the deformed conditions is required. The deformations can be stretching, twisting, bending and elliptic distortions as shown in Fig. 1.

The effects of these deformations on the thermal conductivities of the CNTs were investigated recently [21]. Following this paper, we are going to study the effects of the deformations on the elastic, buckling and vibrational properties of the CNTs in both cantilever and doubly clamped boundary conditions.

2. Modeling and analysis

Fig. 1 schematically shows the discussed deformation in the CNTs [21]. Fig. 1(a) illustrates a normal CNT with normal length and cross section. In this paper, as mentioned earlier, there are CNTs with two cantilever and doubly clamped boundary conditions under the investigation. Fig. 1(b) shows the bending distortion of the CNT and bending angle is illustrated in the figure. The twisted CNT is depicted in Fig. 1(c) and accordingly, the twisting ratio is supposed $\frac{\beta}{Z_0}$. Fig. 1(d) shows the longitudinal or stretching deformation of the CNT. It can be in two tensile and compressive conditions and its ratio is considered $\frac{Z^{\square}}{Z_0}$. The cross sectional (xy) distortion is illustrated in Fig. 1(e). As shown in this figure, the cross section of the CNT changes from a circle to an ellipse. For an xy-distorted nanotube, the ellipse ratio, also called the eccentricity of an ellipse and usually denoted by *e*, is the ratio of the distance between the two foci to the length of one axis, or $e = 2f/2a = f/a = f/y$ [21]. Of course, in this paper, in order to have a better view, we selected x/y as elliptic deformation ratio.

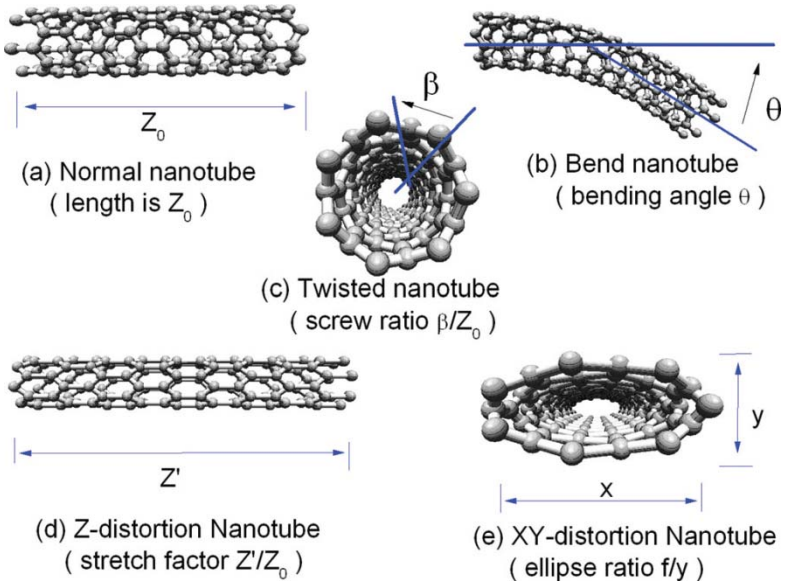

Fig. 1. Possible deformations of the CNTs [21].

To analyze the influences of the deformations on the mechanical properties of the considered CNTs, the well-known molecular mechanics approach is applied. In this approach, a 3D beam element is considered the covalent bond between two carbon atoms. This element can bear axial, bending and torsional loads and hence may be a good choice for our purposes. Its properties are obtained from equalizing the strain energies and C-C bond energies with each other. The obtained properties for the mentioned element are as following:

$$\frac{EA}{L} = k_r \ , \ \frac{EI}{L} = k_\theta \ , \ \frac{GJ}{L} = k_\varphi \ . \tag{1}$$

where E and G are respectively elastic and shear moduli, and A, L, I and J are cross section, length, moment of inertia and polar moment of inertia of the beam element respectively. Furthermore, k_r, k_θ and k_φ are stretching, bending and torsional stiffnesses respectively determined from computational chemistry and should be substituted in the above equation. Their numerical vales are presented in Table 1.

Table 1. Molecular mechanics constants [10]

k_r	6.52e-7 N.nm^{-1}
k_θ	8.76e-10 N.nm.rad^{-2}
k_φ	2.78e-10 N.nm.rad^{-2}
t	0.34 nm

After some algebraic calculations on Eq. (1), the elastic properties of the mentioned beam element with circular cross section are obtained as below [10].

$$d = 4\sqrt{\frac{k_\theta}{k_r}} \ . \tag{2}$$

$$E = \frac{k_r^2 L}{4\pi k_\theta} \ . \tag{3}$$

$$G = \frac{k_r^2 k_\varphi L}{8\pi k_\theta^2} \ . \tag{4}$$

where d is the diameter of the considered element. The numerical values of the elastic properties of the beam element are calculated by replacing the molecular mechanics constants into Eqs. (2-4):

$$d = 0.147 \text{ nm}, \qquad E = 5.49 \text{ TPa}, \qquad G = 0.87 \text{ TPa}$$

These values are fed into the FE program to analyze the elastic, buckling and vibrational behaviors of the considered CNTs.

3. Results and discussion

In this section, the effects of the described deformations on the mechanical behaviors of the CNTs are studied in three distinct sub-sections: elastic modulus, vibrational properties and bucking behaviors.

3.1 Effects of the deformations on the elastic modulus

In this section, only one CNT structure is studied due to the independency of the elastic modulus on the dimensions of the nanotubes. The considered CNT has lengths (Z) 10nm and (10,0) chirality vector. Among the possible distortions for the CNTs, we investigate the effects of stretching, twisting and elliptic deformations on the elastic modulus of the CNTs in this section. In fact, bending deformation distorts the CNT from its straight shape and thus its elastic modulus and buckling behaviors are not studied here due to its curved shape rather than straight one. It is worth noting that bending effects are only investigated on the natural frequencies in the following sub-sections.

To calculate the elastic modulus of the CNT, we apply an axial force on its free end when its other end is constrained as shown in Fig. 2.

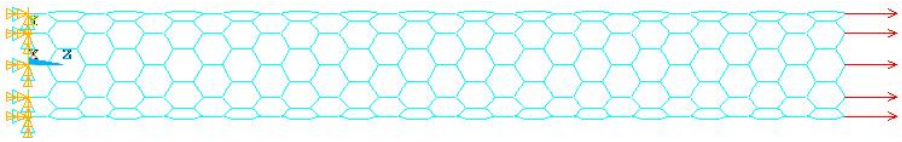

Fig. 2. CNT under a tensile force.

Using Eq. (5), we can obtain the deformation in axial direction and estimate the elastic modulus.

$$E_{CNT} = \frac{N\, L_{CNT}}{\delta\, A_{CNT}} \tag{5}$$

where, E_{CNT}, A_{CNT}, L_{CNT} are respectively the elastic modulus, cross section area and length of the CNT and N and δ are the applied tensile force and deformation caused by this force. The elastic modulus of the CNT is obtained E_{CNT}=1.05 TPa.

Fig. 3 depicts the variation of the CNT elastic modulus vs. stretching ratio. The figure proposes that with increasing the stretching ratio, the elastic modulus does not show any changes. Our simulations offer that this result is generalized to other two deformations. In other words, stretching, elliptic and twisting distortions do not influence the elastic modulus of the CNT effectively.

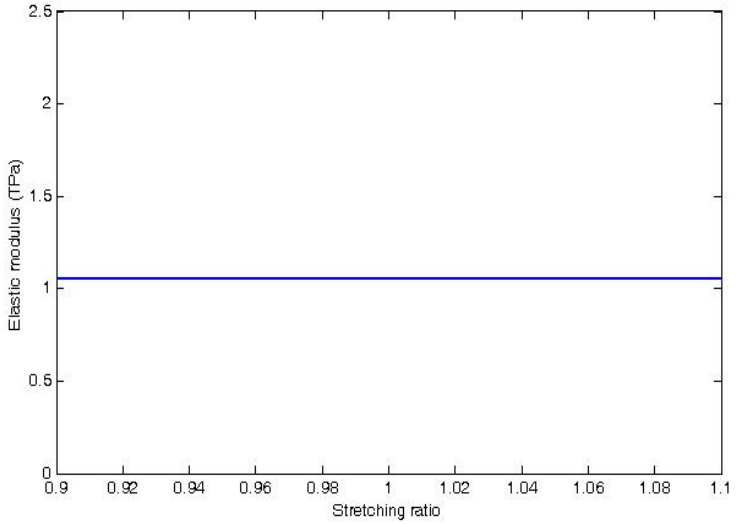

Fig. 3. Effects of stretching ratio on the elastic modulus of the CNTs.

3.2 Effects of the deformations on buckling behaviors

In this section, the considered CNTs have lengths (*Z*) 10nm and (17,0) and (10,0) chirality vectors with two cantilever and doubly clamped boundary conditions. The normal buckling mode shapes of a CNT in two different boundary conditions are shown in Figs. 4 and 5. Fig. 4 devotes to the first boundary condition that is cantilever and Fig. 5 associates with the second boundary condition which is being constrained form the both sides with one exception in the axial direction in one end.

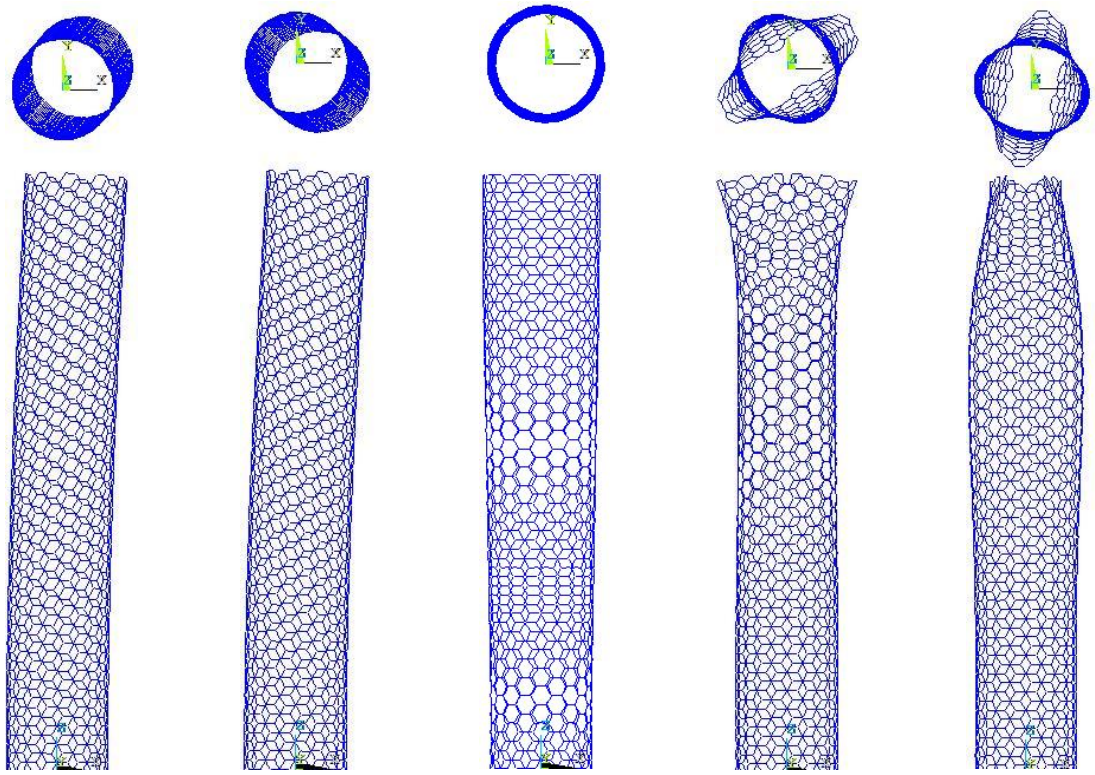

(1) (2) (3) (4) (5)

Fig. 4. Buckling mode shapes of the cantilevered CNT.

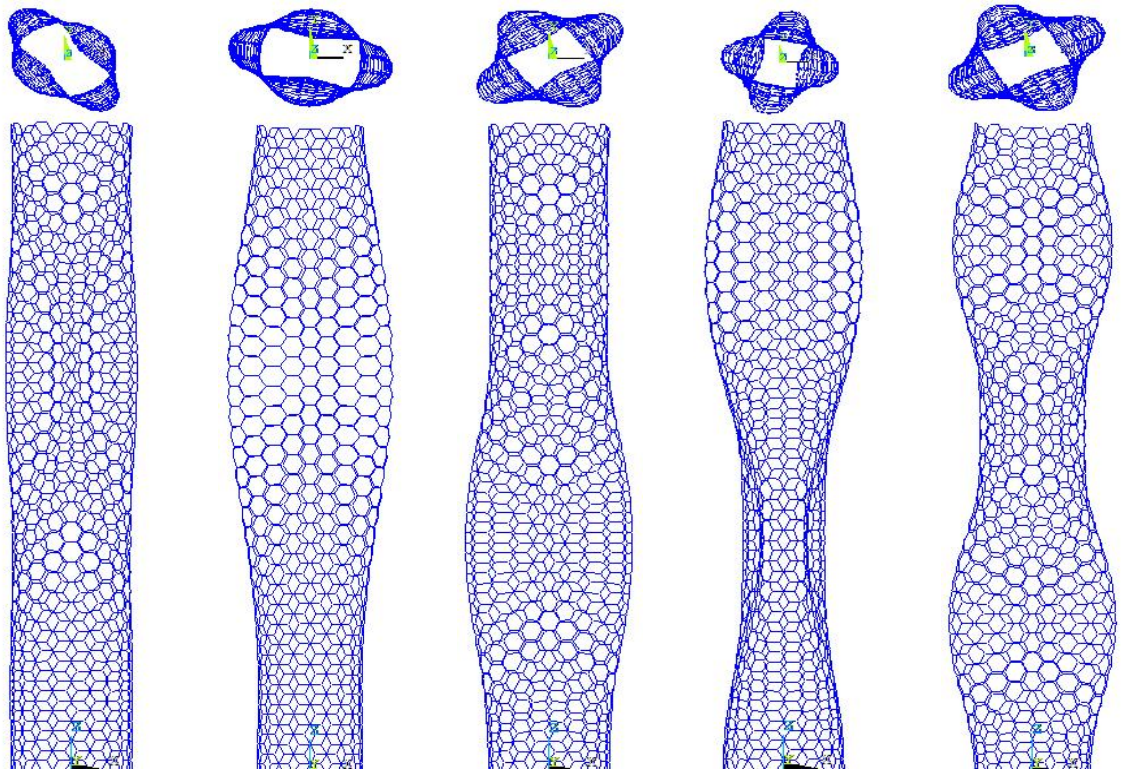

Fig. 5. Buckling mode shapes of the doubly clamped CNT.

Here, we are going to present the results of our modeling related to the effects of the deformations depicted in Fig. 1 on the critical buckling loads. As mentioned before, the effects of bending distortion is not studied here due to its shape distorting from straight position. Fig. 6 shows the effects of elliptic ratio on the buckling critical loads. As shown in this figure, with increasing the elliptic ratio, the critical buckling loads decrease. The gradient of decreasing is larger for (17,0) chirality implying that with increasing the diameter of the CNT, the elliptic ratio affects more remarkably. Furthermore, the figure proposes that the effects of this deformation are stronger for cantilever boundary condition rather than doubly clamped one, especially for larger diameters.

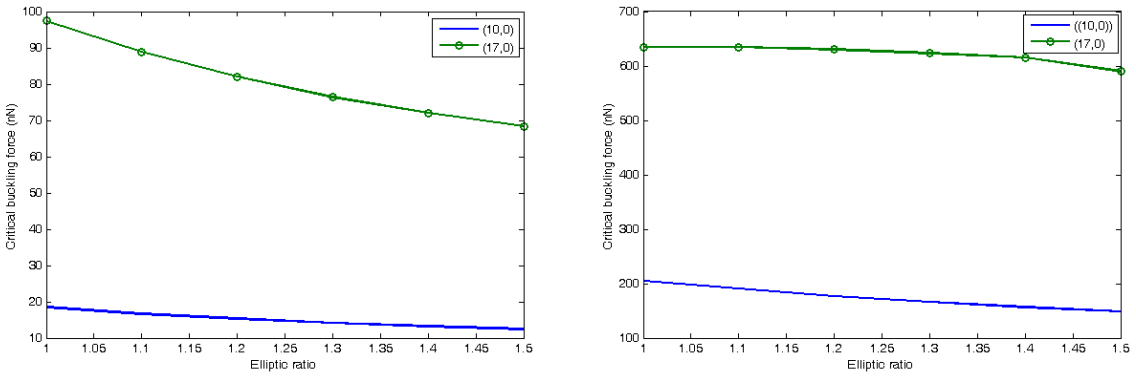

(a) Cantilever boundary condition (b) Doubly clamped boundary condition

Fig. 6. Critical buckling load of the considered CNTs vs. elliptic ratio.

However, our simulations reveal that twisting deformation does not affect the buckling loads effectively if in cantilever or doubly clamped boundary conditions.

On the other hand, the effects of stretching ratio on the buckling loads are presented in Fig. 7. As shown in the figure, with increasing the ratio more than 1 (stretching ratio=1 devotes to the undeformed CNT), the buckling loads decrease in general. In contrast, with decreasing the ratio less than 1, the buckling loads increase. The variations of buckling load values are higher for larger diameters in cantilever and for smaller diameters in doubly clamped boundary conditions.

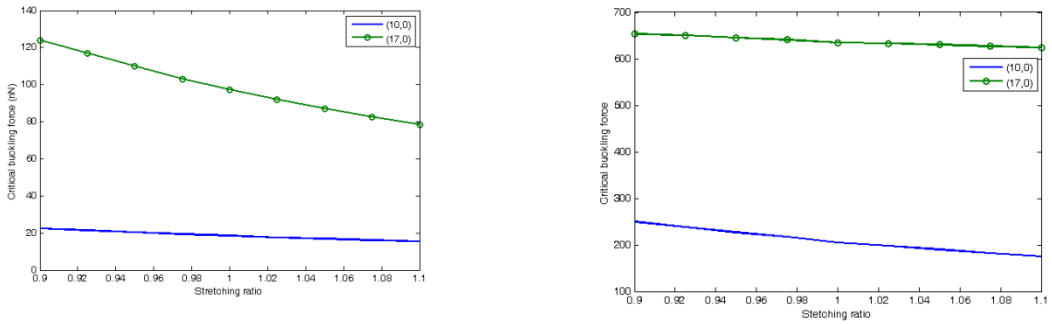

(a) First boundary condition (b) Second boundary condition

Fig. 7. Critical buckling load of the considered CNTs vs. stretching ratio.

3.3 Effects of the deformations on the natural frequencies

In this subsection, the results of deformation effects on the natural frequencies of the CNT are studied. The mode shapes of an undeformed CNT in two cantilever and doubly clamped boundary conditions are illustrated in Figs. 8 and 9. Two CNTs with lengths (Z) 10 nm and (10,0) and (17,0) chirality vectors are considered to investigate the deformation effects. Fig. 10 predicts the effects of the stretching deformation on the first two natural frequencies. It is worth noting that in the normal situation of the CNTs, the first two natural frequencies equal each other in both cantilever and doubly clamped boundary conditions.

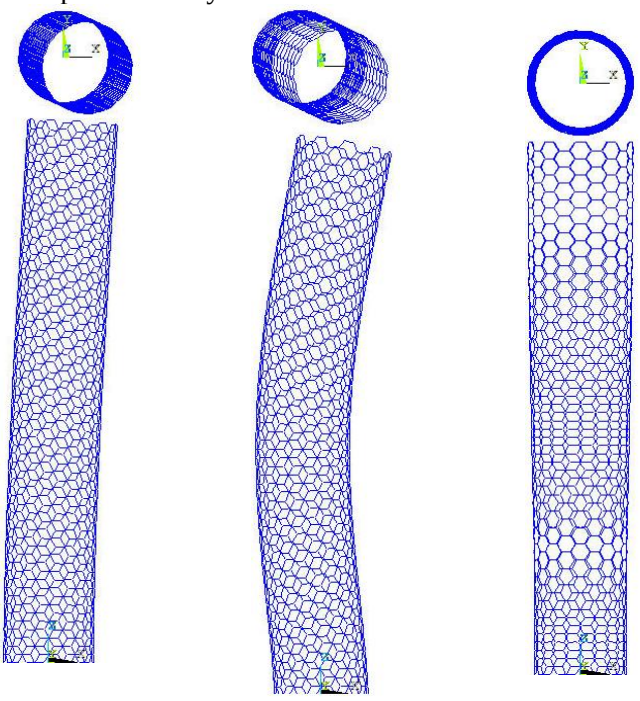

(1,2) (3,4) (5)

Fig. 8. Vibration mode shapes of a cantilever CNT

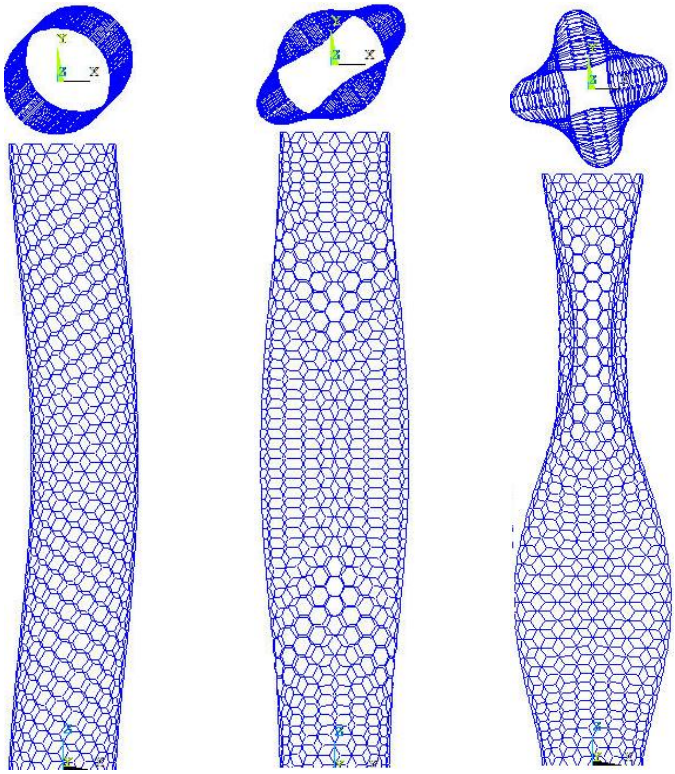

Fig. 9. Vibration mode shapes of a doubly clamped CNT

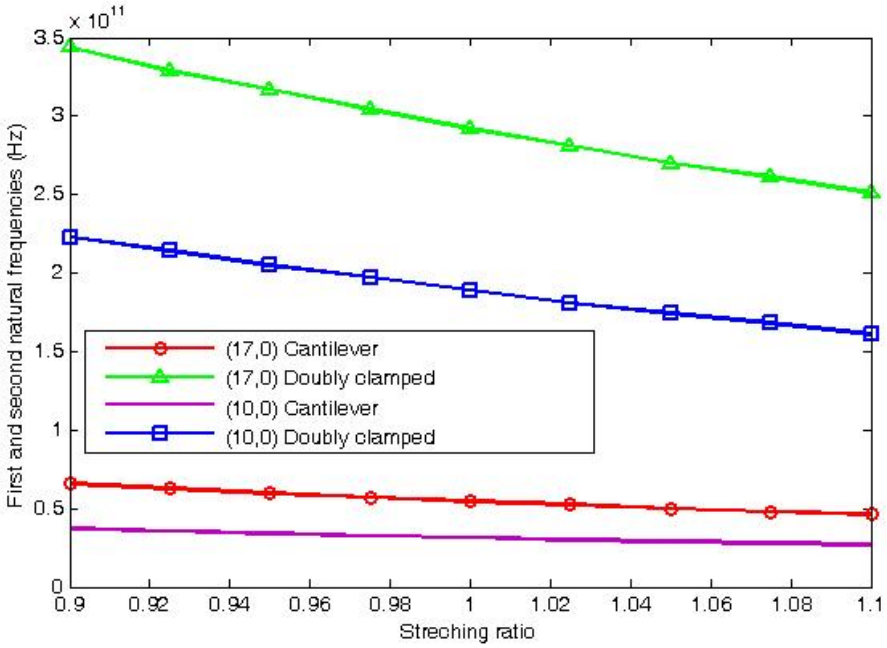

Fig. 10. Longitudinal deformation effects on the natural frequencies.

As shown in this figure, all of the natural frequencies decrease with increasing stretching ratio more than 1 but this decreasing dominates in the doubly clamped boundary conditions. However, for stretching ratios less than 1, the natural frequencies increase. Furthermore, it seems that the longitudinal or stretching deformation has higher effects on the same length CNTs with larger diameters.

On the other hand, Fig. 11 proposes that the twisting deformation does not affect the natural frequencies greatly. It is, of course, in the elastic region and approximately exceeding 1.5

deg/nm leads to the plastic deformations of the CNTs which may have more influential effects. This variation is completely similar to the effects of elastic twisting on the thermal conductivity of the CNTs [21]. The only effect is on the (17,0) doubly clamped boundary condition which this deformation reduces its natural frequency a little. Hence, it may be concluded that this effect appears only in larger diameters.

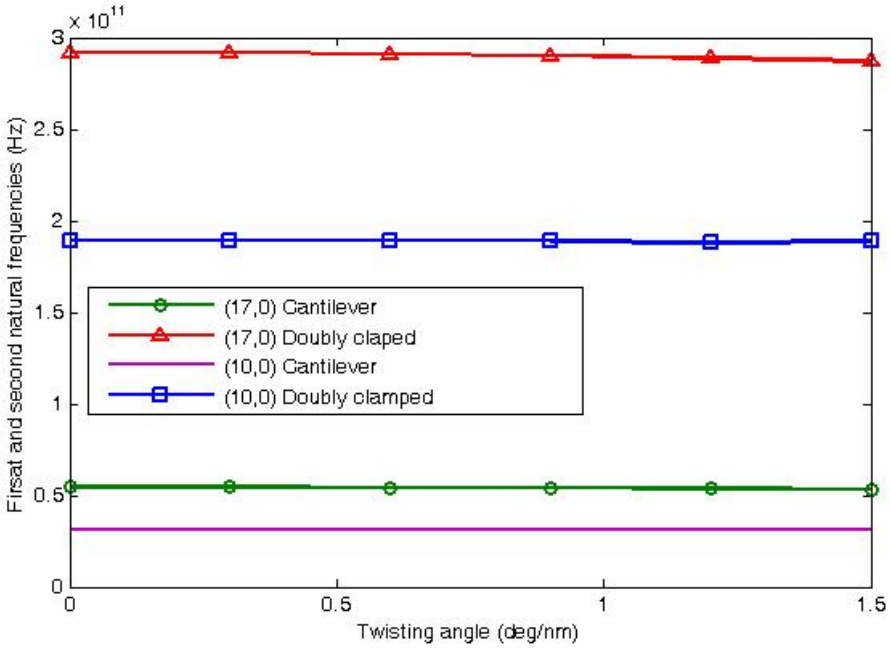

Fig. 11. Twisting deformation effects on the natural frequencies.

Fig. 12 presents the bending effects on the natural frequencies of the CNTs. As shown in this figure, the bending deformation influences the doubly clamped boundary conditions. This is, of course, more considerable for the second modes. Another point to conclude from the figure is that, for doubly clamped CNTs, with increasing bending angle, the first and second natural frequencies diverge from each other while they equal in the normal situations.

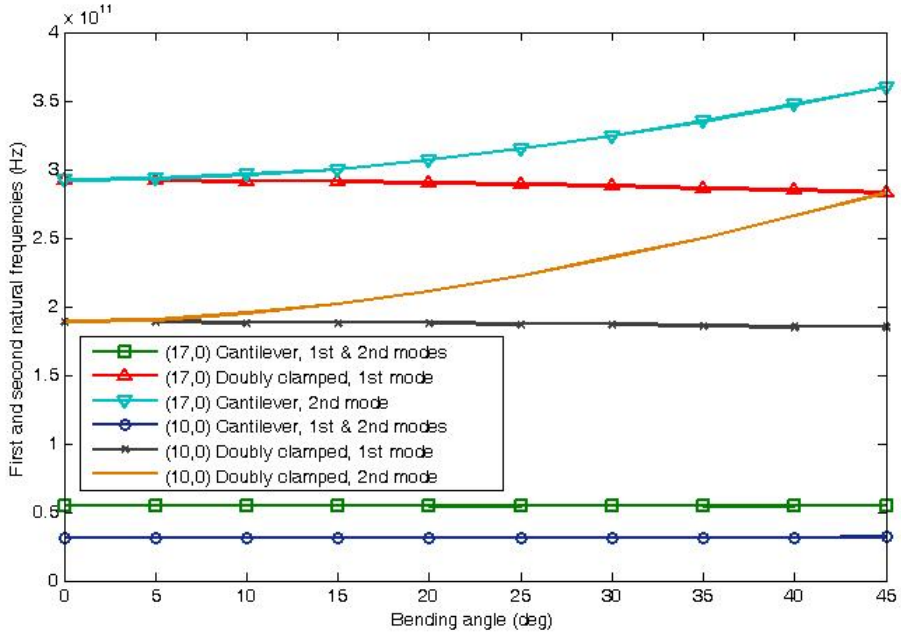

Fig. 12. Bending deformation effects on the natural frequencies.

Finally, the effects of the cross sectional elliptic distortions on the natural frequencies of the CNTs are investigated. Fig. 13 shows the mentioned effects graphically. According to the figure, the cross section deformation has higher influences on the doubly clamped CNTs. This figure proposes that, in all possible conditions, for the elliptic ratios lower than 1, the first frequencies increase while the second ones decrease. On the other hand, for cross section deformation ratios higher than one, the first natural frequencies decrease and the second ones increase. Therefore, unlike the previous cases, this deformation has not even effects.

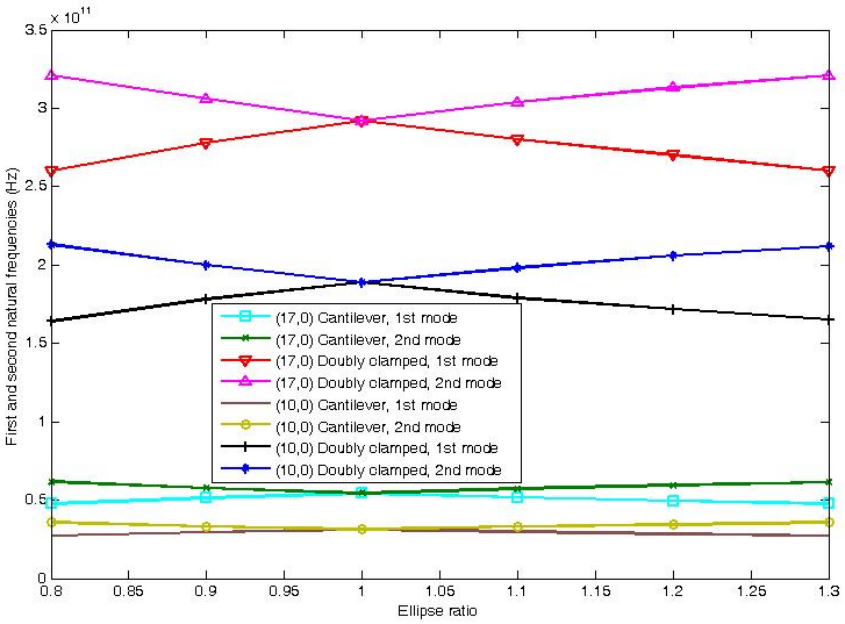

Fig. 13. Elliptic deformation effects on natural frequencies.

4. Conclusion

The paper studied the effects of geometric distortions including stretching, twisting and elliptic deformations on the buckling loads of the CNTs. These deformations and bending distortion were considered to investigate the first two natural frequencies of the deformed CNTs in two cantilever and doubly clamped boundary conditions. The considered CNTs had lengths 10nm and chiralities (10,0) and (10,17) respectively. The results revealed that in vibrational analysis, except twisting deformation, the others affect the values of the frequencies remarkably. This fact can be attributed to the elastic behaviors of the CNTs and it seems that with increasing twisting ratio, the CNT shows plastic behavior and the natural frequencies change. This matter can be studied in the future studies.

References

[1] M. L. Chen, F. J. Zhang, and W. C. Chun, New Carbon Mat **24**, 159 (2009).
[2] X. Zhang, C. Zhu, Field-emission lighting tube with CNT film cathode, Microelec **37**, 1358 (2006).
[3] L. L. Ke, J. Yang, S. Kitipornchai, J. Compos. Struct **92**, 676 (2010).
[4] H. L. Lee, W. J. Chang, J. Phys. E **41**, 529 (2009).
[5] X. Q. He, S. Kitipornchai, K. M. Liew, J. Mech. and Phys. of Solids **53**, 303 (2005).
[6] Y. Wang, X. Wang, X. Ni, H. Wu, Comput. Mat. Sci **32**, 141 (2005).
[7] S. K. Georgantzinos, N. K. Anifantis, Comput. Mat. Sci **47**, 168 (2009).
[8] G. Yun, H. S. Park, J. of Comput. Meth. in Appl. Mech. Eng **197**, 3324 (2008).
[9] M. Aydogdu, J. Mech. Sci **50**, 837(2008).
[10] A. Sakhaee Pour, M. T. Ahmadian, A. Vafai, J. Thin-Walled Struct **47**, 646 (2009).

[11] S. B. Legoas, V. R. Coluci, S. F. Braga, P. Z. Coura, S.O. Dantas, D. S. Galvao, Phys. Rev. Lett **50**, 055504 (2003).
[12] C. Li. T. W. Chou, Appl. Phys. Lett **84**, 5246 (2004).
[13] B. Li, and T. Chang, J. Appl. Phys **108**, 054304 (2010).
[14] M. H. Mahdavi, L. Y. Jiang, X. Sun, J. Appl. Phys **106**, 114309 (2009).
[15] H. L. Lee, and W. J. Chang, J. Phys. E **41**, 529 (2009).
[16] C. Li, E. T. Thostenson, T. W. Chou, J. Compos. Sci. and Tech **68**, 1227 (2008).
[17] S. B. Tooski, J. Appl. Phys **109**, 014318 (2011).
[18] M. Nosrati, S. Jalili, R. Sahraei, Digest J. Nanomat. and Biostruct **6**, 1403 (2011).
[19] J. Yazdani, A. Bahrami, Digest J. Nanomat. and Biostruct **4**, 369 (2009).
[20] Z. H. Khan, M. S. Ansari, N. A. Salah, A. Memic, S. Habib, M. S. Shahawi, Digest J. Nanomat. and Biostruct **6**, 1947 (2011).
[21] W. R. Zhong, M. P. Zhang, D. Q. Zheng, B. Q. Ai, J. Appl. Phys **109**, 074317 (2011).